文章编号　2095-1531(2018)03-0420-11

Synthesis of chitosan-based polymer carbon dots fluorescent materials and application of self-assembled drug-loading

YU Shu-juan*, CHEN Kuan, WANG Feng, ZHU Yong-fei
(*College of Chemistry and Material Science, Guangxi Teachers Education University, Nanning* 530001, *China*)
* *Corresponding author, E-mail: ysj*2007@126. *com*

Abstract: Fluorescent carbon dots have the advantages of good chemical stability, low toxicity, and surface functionalization, which has caused concern. In recent years, polymer carbon dots synthesize by polymer polysaccharides have become a new research hotspot. In this paper, a chitosan-based fluorescent polymer carbon dot material is synthesized by hydrothermal method and used for drug-loading research. We choose chitosan-graft-polyethylene glycol monomethyl ether and citric acid derivatives as the carbon sources for the carbon dots, because chitosan and polyethylene glycol are both a carbon source for carbon dots and a passivation reagent for carbon dots. Then the quantum yield of the polymeric carbon dots is increased. Polymer carbon dots can also retain the molecular structure of polyethylene glycol and chitosan, providing favorable conditions for its application in drug loading. The structural characterization is performed on P(CS-g-mPEG-CA)CDs by IR, UV, X-ray diffraction, photoelectron spectroscopy, transmission electron microscopy and photoluminescence spectra and pH stability test is carried out. The results show that the synthesized P(CS-g-mPEG-CA)CDs has higher fluorescence quantum yield(66. 81%), longer fluorescence lifetime(15. 247 ns), and better pH stability. Using Doxorubicin as a model drug, a load study was conducted using this polymer carbon dot. The results show that if the degree of substitution of mPEG is 11. 9%, the maximum loading rate of polymer carbon dots is 51. 3% and the maximum drug release rate is 28. 7%. In addition, we also found that drug loading and release could be controlled by the grafting rate of mPEG. In addition, the cytotoxicity of polymer carbon dots on nasopharyngeal carcinoma cells(CNE-2) is evaluated using an MTT assay. The study shows that there is no obvious cytotoxicity of blank P(CS-g-mPEG-CA)CDs, and that the survival rate of CNE-2 cells decreases with the increase of drug-loaded micelles. The results show that the P(CS-g-mPEG-CA)CDs have a certain application prospect in the aspects of fluorescence labeling, drug delivery, fluorescent tracer system and controlled release.

Key words: chitosan; polymer carbon dots; citric acid; fluorescent materials; drug loading; mPEG; doxorubicin

收稿日期:2018-01-11;**修订日期**:2018-02-09
基金项目:广西自然科学基金项目(No. 2016GXNSFAA380203)
Supported by Natural Science Fund of Guangxi Province of China(No. 2016GXNSFAA380203)

壳聚糖基聚合物碳点荧光材料合成及其自组装载药应用

于淑娟*, 陈　宽, 汪　丰, 朱永飞
(广西师范学院 化学与材料科学学院, 广西 南宁 530001)

摘要: 荧光碳点具有化学稳定性好、毒性小、可表面功能化等优点, 引起了人们极大的兴趣。近年来, 由高分子多糖合成的聚合物碳点成为另一研究热点。本文通过水热法合成了一种壳聚糖基荧光聚合物碳点材料(P(CS-g-mPEG-CA)CDs), 并用于载药研究。基于壳聚糖和聚乙二醇既是碳点的碳源也是碳点的钝化试剂, 本文选择壳聚糖接枝聚乙二醇单甲醚和柠檬酸衍生物作为聚合物碳点的碳源, 以提高聚合碳点的量子产率。另外, 聚合物碳点还可以保留聚乙二醇与壳聚糖分子结构, 为其在载药方面的应用提供有利条件。采用红外光谱、紫外光谱、X 射线衍射、光电子能谱、透射电子显微镜和光致发光光谱对 P(CS-g-mPEG-CA)CDs 进行了结构表征以及 pH 值稳定性的测试。结果表明, 所合成的 P(CS-g-mPEG-CA)CDs 具有较高的荧光量子产率(66.81%)、较长的荧光寿命(15.247 ns)、良好的 pH 稳定性。以阿霉素为模型药物, 利用该聚合物碳点进行了负载研究, 结果表明, 当聚乙二醇单甲醚取代度为 11.9% 时, 聚合物碳点的载药量最高为 51.3%, 最大药物释放率为 28.7%, 此外, 药物的装载和释放可以通过 mPEG 的接枝率进行控制。采用 MTT 法评价了聚合物的碳点对鼻咽癌细胞(CNE-2)的毒性作用。研究表明, 空白聚合物碳点无明显细胞毒性, CNE-2 细胞存活率随着载药胶束的增加而降低, 说明载药胶束对 CNE-2 细胞有较强的抑制作用。可见该 P(CS-g-mPEG-CA)CDs 在荧光标记、药物递送、荧光示踪系统和控制释放方面, 具有一定的应用前景。

关　键　词: 壳聚糖; 聚合物碳点; 柠檬酸; 荧光材料; 载药; 聚乙二醇单甲醚; 阿霉素
中图分类号: O613.71; TB383　　**文献标识码:** A　　doi: 10.3788/CO.20181103.0420

1　Introduction

Carbon dots (CDs) are a class of nanomaterials that have recently attracted attention due to their fascinating properties, including high photostability against photobleaching and blinking, good biocompatibility[1], low cytotoxicity[2], and excellent photoluminescence[3-4]. Compared with conventional fluorescent dyes, carbon-based fluorescent materials are advantageous since they are easily synthesized from a wide range of raw materials, such as citric acid (CA), glucose, milk, and oranges[5-7]. They have a wide range of applications in chemosensors, electroluminescent devices, catalysis, biological markers in the biomedical field and other areas[8-10]. Recent studies indicated that some non-conjugated polymers were inherently emissive[11-13]. Despite the absence of common fluorophores, these materials were still highly emissive in solution. Fluorescent polymeric carbon dots (PCDs) prepared from non-conjugated linear polymers have the advantages of being easily purified compared to CDs, and retaining functional groups on the polymer that are susceptible to molecular modification, giving them better water solubility than conjugated polymer fluorescent materials. In recent years, there has been increasing studies on the synthesis of PCDs using chitosan as the raw material and further expanding their application. For example, Yang *et al.*[14], used chitosan (CS) as a carbon source to synthesize chitosan-based carbon dots (CS-CDs) with hydrothermal method. The CS-CDs had a fluorescence quantum yield (QY) of 7.8% and were successfully applied to biological imaging

of cancer cells in the human lung. Subsequently, Xiao *et al.*[15], synthesized CS-CDs by microwave irradiation, and the QY was 6.4%. Wang *et al.*[16], also used CS as raw material to synthesize CS-based composite carbon dots and studied their applications as fluorescent films, fluorescent coatings and in cell imaging. Zu *et al.*[17], synthesized multicoloured fluorescent nanostructures for the imaging of small aquatic craniate animals with chitosan and starch as raw materials. These promising findings inspire further investigation of the application of CS-CDs. However, the QY of most of the CS-CDs were relatively low, so there were few active sites and the selectivity was poor in these studies[18]. These deficiencies will severely limit the widespread use of CS-CDs, so the preparation of polymer carbon dots with high QY, together with further exploration of their applications, is of great importance.

Over the years, fluorescent nanoparticles(NPs) have been much studied, especially those that are biocompatible. They are extremely useful for monitoring transport within cells and tissues, identifying disease sites and determining therapeutic response[19]. For instance, cellular internalization, intracellular trafficking and *in vivo* biodistribution of fluorescent NPs can be conveniently monitored using fluorescence microscopy[20-21]. Current methods of preparing fluorescent NPs include conjugating or encapsulating organic dyes or utilizing inorganic fluorescent NPs such as quantum dots(QDs) or other metal particles[22-23]. However, there are various limitations to these common approaches. For instance, the organic dyes conjugated onto or encapsulated into the NPs may dissociate from the NPs. Moreover, polymers used for encapsulation often lead to disappearance of the fluorescence of QDs[24]. Inorganic fluorescent NPs such as QDs can have high cytotoxicity, which limits their use as drug nanocarriers, and may also require complicated synthetic procedures.

Due to the above shortcomings, in this work we synthesized polyethylene glycol chitosan derivatives (CS-g-mPEG) using CS and PEG, molecules that have been widely used in drug-delivery, as raw materials[25]. Then, CA was grafted onto CS-g-mPEG under mild conditions. Finally, a chitosan-based polymer carbon dot(P(CS-g-mPEG- CA)CDs) fluorescent material with high fluorescence QY and long fluorescent lifetime was synthesized using a hydrothermal method after adding the nitrogen doping reagent N-(2-hydroxyethyl) ethylenediamine. The solution properties of the polymer carbon dots indicated that the P(CS-g-mPEG-CA)CDs could self-assemble into micelles. We prepared water-soluble drug-loaded nanoparticles, (P(CS-g-mPEG-CA)CDs/DOX), using doxorubicin (DOX) as the model drug, and studied drug loading and drug release performance. The toxicity and antitumor effect of P(CS-g-mPEG-CA)CDs were evaluated by MTT assay.

2 Materials and methods

2.1 Materials

Chitosan was provided by Zhejiang Aoxing Biochemical Technological Co. Ltd. (China) with a deacetylation degree of 97% and a viscosity average molecular weight of 25 kDa. Doxorubicin hydrochloride(DOX HCl, 98% purity), poly(ethylene glycol) methyl ether acrylate with molecular weight 2 000 g/mol(mPEGEA) and 3-(4,5-dimeth-ylthiazol-2-yl)-2, 5-diphenylterazolium bromide (MTT) were purchased from Aladdin Chemical Reagent Co, Ltd. (Shanghai, China). The other reagents, including dichloromethane, triethylamine, citric acid (CA), ceric ammonium nitrate(CAN), acetone, 1-ethyl-3-(3-dimeth-ylaminopropyl) carbodiimide hydrochloride (EDC), N-hydroxysuccini-mide (NHS) and N-(2-hydroxyethyl) ethylenediamine (NHEA) were of analytical grade and were supplied by Sinopharm Chemical Reagent Co, Ltd, Shang-

hai, China. All commercially available solvents and reagents were used without further purification. CS-g-mPEG and CS-g-mPEG-CA were synthesized by reference [26] and [27] respectively.

2.2 Preparation of P(CS-g-mPEG-CA)CDs

Anhydrous CA (0.25 g), CS-g-mPEG-CA (0.25 g), NHEA (1 mL), and deionized water (8 mL) were added to a Teflon-lined stainless steel autoclave with a capacity of 25 mL. The autoclave was heated at 180 ℃ for 3 h and then cooled to room temperature. The resultant light yellow solution was separated by centrifugation at 10 000 rpm for 30 min. The supernatant was then loaded into dialysis bags (dialysis bag MWCO = 8 000 – 14 000 Da) for dialysis against deionized water for 3 days, followed by freeze-drying to obtain pure P(CS-g-mPEG-CA)CDs.

The QY of P(CS-g-mPEG-CA)CDs was determined by using quinine sulfate (literature $\Phi = 0.54$ in 0.05 M H_2SO_4 at 360 nm) as a standard[28].

2.3 Preparation of Drug-loaded Micelles

The incorporation of DOX · HCl into P(CS-g-mPEG-CA) CDs self-assembled micelles was achieved using an ultrasonic method[29]. Briefly, DOX · HCl (50, 150, 250, 450 or 650 μg) was dissolved in dichloromethane (DCM, 10 mL) and ultrasonicated for 2 h to obtain a DOX dispersion. The P(CS-g-mPEG-CA)CDs was dissolved in a 1% acetic acid solution. The DOX HCl dispersion in DCM (10 mL) was added to the P(CS-g-mPEG-CA)CDs acetic acid solution (1 mL). Drug-loaded micelles (P(CS-g-mPEG-CA)CDs/DOX) were obtained by sonication for 30 min and adjustment to pH 7. Blank micelles were also prepared in the same way, but without the addition of DOX. The resultant products were subjected to analysis and testing. All operations were carried out in a dark environment.

The synthesis of P(CS-g-mPEG-CA) CDs and its drug loading route to DOX are shown in Fig. 1.

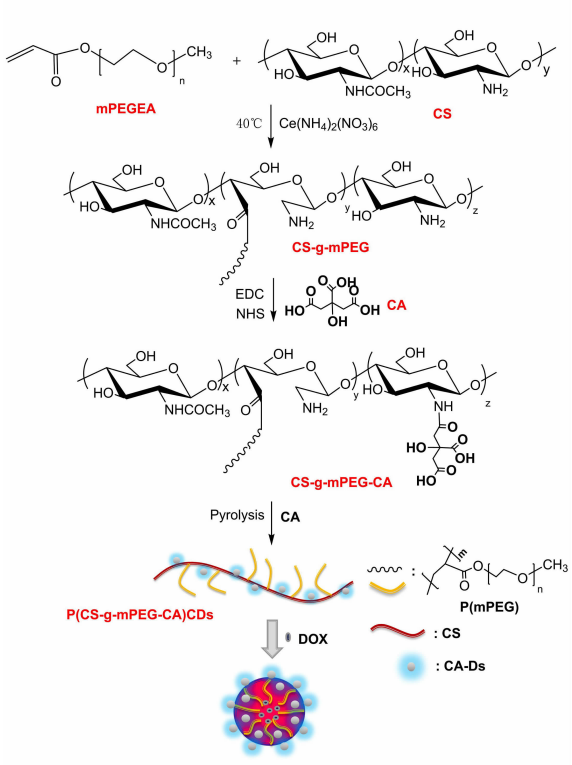

Fig. 1　Illustration of the formation of P(CS-g-mPEG-CA)CDs from CS, mPEGEA and CA via a hydrothermal approach and the drug-loaded micelles

2.4 Characterization

Fourier transform infrared (FTIR) spectra were recorded on a FTIR spectrometer (Paragon 1000, Perkin Elmer, USA). The photoluminescence spectra of the samples were obtained using a spectrofluorometer (RF-5301PC, Shimadzu, JP). The morphologies of all samples were characterized by high resolution transmission electron microscopy (HR-TEM, Tecnai G2 F30 S-TWIN, FEI, USA). UV-vis absorption spectra of the samples were obtained with a UV-vis spectrophotometer (Varian Cary 100 SCAN, Agilent Technologies Inc., Santa Clara, CA, USA). X-ray diffraction (XRD) patterns of CS, CS-g-mPEG-CA and P(CS-g-mPEG-CA)CDs powder were recorded on a diffractometer (D/max 2400, Rigaku Corporation, Tokyo, Japan) operating at 40 kV and 40 mA at 25 ℃. The scanning scope

was from 10° to 40°(2θ) and the scanning rate was 4°/min. Luminescence lifetimes were measured using a fluorescence spectrometer(Fluorolog-3, Horiba Jobin Yvon Inc., France). X-ray photoelectron spectra(XPS) were collected using an X-ray photoelectron spectrometer (ESCALAB250, Thermo, UK).

3 Results and discussion

3.1 FTIR Spectroscopy

The FTIR spectra of CS-g-mPEG(a), CS-g-mPEG- CA(b), and P(CS-g-mPEG-CA) CDs(c) are shown in Fig. 2. A very strong broad peak at around 3 432 cm^{-1} in the spectrum of CS-g-mPEG can be attributed to the stretching vibrations of CS-NH_2 and –OH groups. The peak at 2 884 cm^{-1} is attributed to the mPEG C–H stretching vibration. The peaks at 1 718 and 1 641 cm^{-1} can be assigned to the CS-g-mPEG C=O stretching and CS-NH_2 scissoring vibrations, respectively. The band observed at 1 112 cm^{-1} is due to the C–O–C stretching vibration of CS glycosidic linkages and mPEG. The broadened peak at around 3 405 cm^{-1} in the spectrum of CS-g-mPEG-CA could be due to the stretching vibration of CA O–H, and the extension vibration of CS N–H, and intermolecular hydrogen bonds of CS and CA. The amide I band appearing at 1 641 cm^{-1} is associated with the C=O stretching vibrations and the amide II band at 1 532 cm^{-1} is associated with the C–N stretching and N–H vibration. These results indicated that the CS-g-mPEG-CA was successfully prepared. It is apparent that the FTIR spectrum of P(CS-g-mPEG-CA) CDs contains characteristic absorption bands of CS and mPEG, but not of CA. This indicates that the CS and mPEG fragments are preserved during hydrothermal treatment while most of the CA is carbonized.

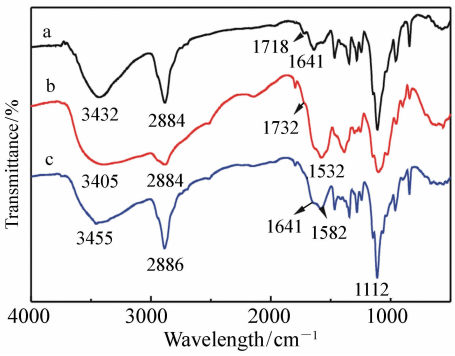

Fig. 2 FT-IR spectra of CS-g-mPEG(a), CS-g-mPEG-CA(b) and P(CS-g-mPEG-CA) CDs(c)

3.2 XRD Analysis

As shown in Fig. 3, the XRD pattern of CS showed characteristic peaks at 20.2°, indicating a high degree of crystallinity. Modification of CS with mPEG and CA produced two narrow peaks at 19.18° and 23.40° in the XRD pattern of CS-g-mPEG-CA, which coincided with the diffraction peaks of mPEG crystals and thereby demonstrated the presence of crystalline phases of mPEG in the copolymers. Furthermore, these peaks were clearly different from the crystalline peaks of CS, suggesting that the crystal structure of the grafted compound was disrupted. This probably results from disruption of intermolecular hydrogen bonds between CS units by PEG as previously reported [30]. Compared to CS-g-mPEG-CA, the crystallization peak of P(CS-g-mPEG-CA) CDs was relatively unchanged, but the intensity of the peak increased slightly, indicating that the structure of the main chain was not further damaged after pyrolysis of CS-g-mPEG-CA. In addition, the presence

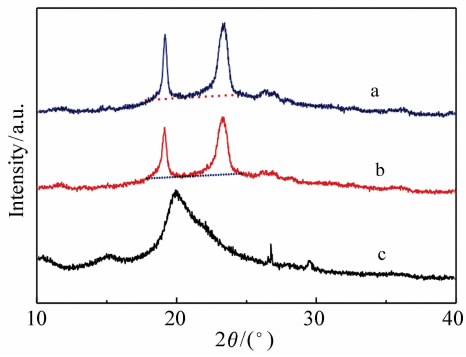

Fig. 3 XRD patterns of P(CS-g-mPEG-CA) CDs(a), CS-g-mPEG-CA(b) and CS(c)

of crystalline peaks of PEG showed that the molecular chains of PEG were not broken down, which also provides favorable conditions for the application of the P(CS-g-mPEG-CA)CDs.

3.3 XPS Study

The surface composition and chemical environments of the as-synthesized P(CS-g-mPEG-CA)CDs were determined using XPS. In the XPS survey spectrum of P(CS-g-mPEG-CA)CDs, the peaks at 287.42, 400.42, and 535.42 eV correspond to C1s, N1s, and O1s, respectively, as shown in Fig. 4a. This result indicated that the P(CS-g-mPEG-CA)CDs was composed of carbon, nitrogen, and oxygen at atomic percentages of 64.49%, 2.87%, and 32.64%, respectively. From the high resolution spectrum of the C1s region (Fig. 4b) three surface components could be assigned, corresponding to C–C at a binding energy of 286.2 eV, together with C–O and C–N at 286.8 eV. In the N1s spectrum, the peaks at 400.1 and 401.7 eV were attributed to nitrogen doped by the NH_2 of the chitosan molecular chain, corresponding to C–N and N–H, respectively (Fig. 4c). The O1s spectrum also contained two peaks, at 532.8 and 533.4 eV, assigned to C–OH/C–O–C and C=O, respectively (Fig. 4d).

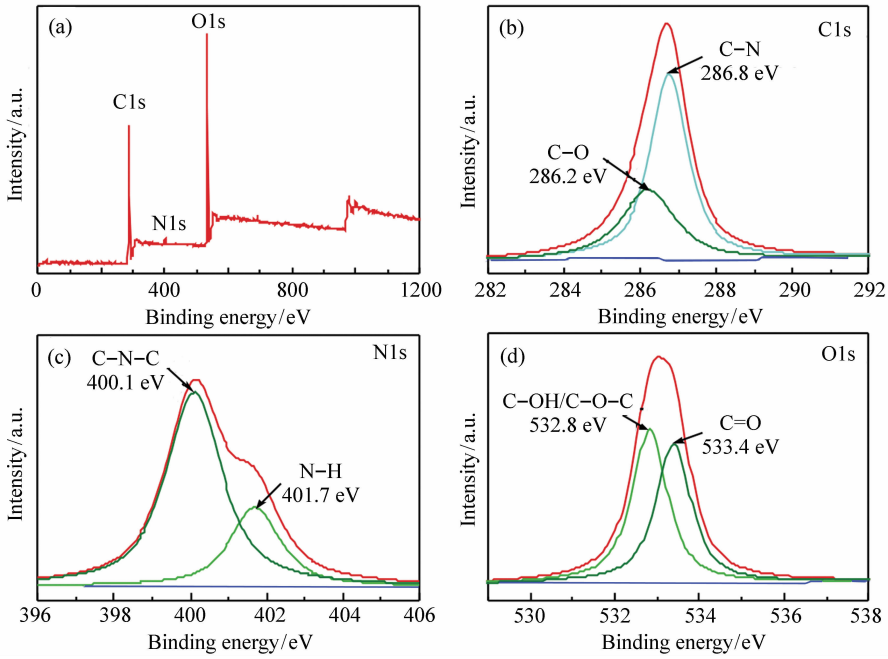

Fig. 4　XPS survey spectrum of P(CS-g-mPEG-CA)CDs (a); High resolution XPS spectrum of C1s region (b); High resolution XPS spectrum of N1s region (c); High resolution XPS spectrum of O1s region (d)

3.4 Analysis of UV-vis and Fluorescence Spectra of P(CS-g-mPEG-CA)CDs

The UV-vis absorption spectrum (Fig. 5A) showed strong peaks at 231 and 357 nm, attributed to the π-π^* transition of C=C and the n-π^* transition of C=O or C–OH bonds, respectively[31-32]. In the PL spectrum (Fig. 5A), the P(CS-g-mPEG-CA)CDs in aqueous solution exhibited excitation and emission wavelengths at 375 and 462 nm, respectively. The solution was a light yellow color under ambient light (Fig. 5A-a), which became bright blue under a hand-held UV lamp (Fig. 5A-b). The aqueous solution of P(CS-g-mPEG-CA)CDs exhibited excitation- independent PL behavior (Fig. 5B). When the excitation wavelength was changed from 280 to 420 nm, the corresponding PL emission peaks for P(CS-g-mPEG-CA)CDs were not significantly shifted. This behavior is a consequence of the

surface/molecular state and particle size distribution of the carbon dots[30]. The fluorescence lifetimes of P(CS-g-mPEG-CA) CDs with different degrees of substitution are shown in Fig. 5C. It can be seen that the fluorescence lifetimes of P(CS-g-mPEG-CA) CDs I, II and III were 14.399, 14.936, and 15.247 ns, respectively. Higher fluorescence lifetimes are attributed to the contribution of nitrogen atoms from doping reagents and chitosan NH_2. The induction of longer average lifetimes by nitrogen atoms may be due to suppression of non-radiative energy transitions in P(CS-g-mPEG-CA) CDs[33]. The relative fluorescence QY values of P(CS-g-mPEG-CA) CDs were measured by the linear slope method (using quinine sulfate as a reference). As shown in Fig. 5D, the QY values of P(CS-g-mPEG-CA) CDs I, II and III were 26.93%, 31.53% and 66.81%, respectively. The QY increased as the degree of mPEG grafting increased, which may be because the polyethylene glycol molecule has a certain passivation effect on the polymer carbon dots[36]. These values are much higher than for chitosan-based carbon dots[15-16]. This enhancement is due to co-passivation of the PCD by CS, PEG molecular chains and nitrogen dopants, which increases the surface defects. In addition, CS and PEG can also be used as carbon sources[15,34], so P(CS-g-mPEG-CA) CDs exhibits higher QY. It is worth mentioning that P(CS-g-mPEG-CA) CDs is a solid powder with excellent storage stability, and its QY was unchanged a year later. The good stability of the P(CS-g-mPEG-CA) CDs, high QY and long fluorescent lifetime provide a broader scope for its application. Further, we also investigated the influence of the solution pH on the fluorescence intensity of P(CS-g-mPEG-CA) CDs. It was found that the fluorescence intensity of the carbon dots first increased and then decreased as the pH value increased, and the fluorescence intensity was highest when pH = 7 (Fig. 5E). It can be seen that changes in the fluorescence intensity were small at pH values from 3 to 11, which indicates that P(CS-g-mPEG-CA) CDs has high fluorescence stability in this range. Good fluorescence stability also provides a basis for application in the pH = 4 –

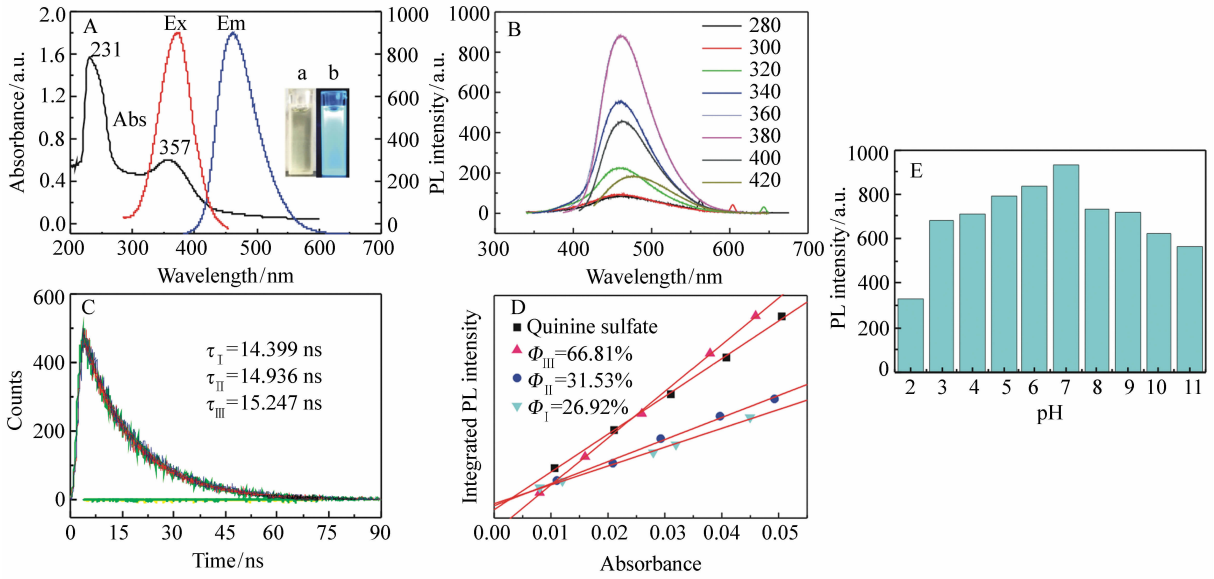

Fig. 5 UV-Vis spectrum and the maximum PL excitation and emission spectra of P CS-g-mPEG-CA) CDs in water and their digital photographs (a) under daylight and UV light (b) (A); PL emission spectra of P(CS-g-mPEG-CA) CDs under different wavelength excitations (B); Fluorescence lifetime (C) and fluorescence quantum yield (QY) (D) of the P(CS-g-mPEG-CA) CDs I, II, and III; Effect of the pH on the P(CS-g-mPEG-CA) CDs fluorescence, (all of the experiments were excited at 360nm) (E)

10 physiological range. This is critically important for practical fluorescent drug carrier applications.

3.5 TEM of P(CS-g-mPEG-CA) CDs Before and After Drug Loading

Fig. 6a shows a representative TEM image of P(CS-g-mPEG-CA) CDs dispersed in water. It can be seen that the formed P(CS-g-mPEG-CA) CDs was mostly present as uniformly dispersed spherical dots, with a particle size of about 3 – 4 nm without apparent aggregation. The morphology of the micelles after drug loading was still spherical, with a particle size of about 60 70 nm which was significantly higher than that of the P(CS-g-mPEG-CA) CDs. as shown in Fig. 6b. This was attributed to the successful loaded of DOX. In addition, the carboxyl groups, Amino groups and hydroxyl groups tended to self-assemble in aqueous solution to form larger size nanoparticles[35].

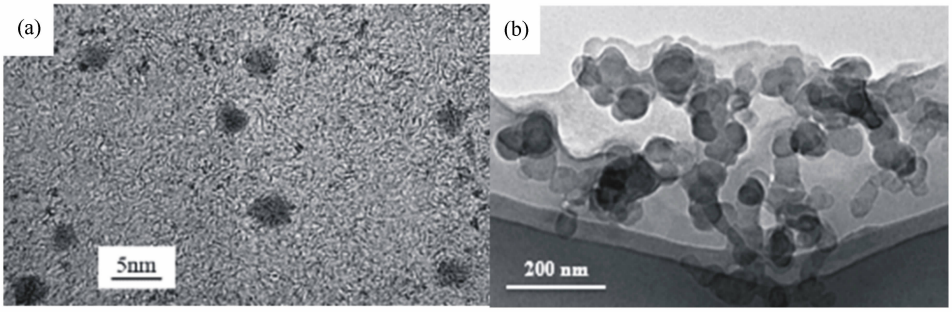

Fig. 6　TEM of P(CS-g-mPEG-CA) CDs(a) and HRTEM of the P(CS-g-mPEG-CA) CDs/DOX(b)

3.6 Drug Release Properties of Drug-Loaded Micelles (P(CS-g-mPEG-CA) CDs/DOX)

DOX was successfully loaded into P(CS-g-mPEG-CA) CDs to give P(CS-g-mPEG-CA) CDs/DOX. Drug loading(DL), entrapment efficiencies (EE) and CMC values are shown in Tab. 1. It can be seen that the DL and EE increased as the mPEG substitution degree increased, due to the decreased intramolecular hydrogen bonding of chitosan at higher mPEG substitution, which is beneficial for the drug DOX/chitosan combination. The in vitro cumulative release of DOX from self-assembled micelles was carried out in PBS(pH 7.4) at 37.8 ℃ and the results are shown in Fig. 7. P(CS-g-mPEG-CA) CDs/DOX displayed an initial fast release followed by a slow phase that was similar to a two-phase pattern[36]. In the early stage of drug release, drug-loaded micelles of P(CS-g-mPEG-CA) at different PEG grafting ratios showed rapid release of drug. After 24 h, drug release was slow, and the total drug released reached only 28.7% (III), 27.6% (II) and 22.9% (I) within 400 h. The rate of release from the drug carrier increased at higher PEG grafting ratio. This is a consequence of the higher proportion of PEG molecules, resulting in increased hydrophilicity and degradation rate of the micelles, thereby increasing the drug release rate. It can be seen that the rate of drug release can be controlled by the degree of grafting of mPEG.

Tab. 1　Elemental analysis data, critical micelle concentration, DL and EE for different micelles

Samples	C/N	DS[a] of mPEG/%	DL/%	EE/%	CMC/(μg · mL^{-1})
I	7.99	4.4	47.9	35.7	0.831 8
II	10.52	8.2	49.4	39.6	5.623 4
III	12.96	11.9	51.3	40.8	8.317 6

[a] DS: degree of substitution.

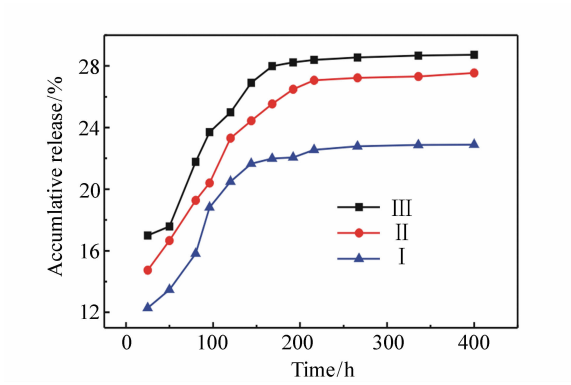

Fig. 7 In vitro release of DOX from P(CS-g-mPEG-CA)CDs micelles in the PBS(pH 7.4)

3.7 In Vitro Cytotoxicity Analysis

For the cell viability test, human nasopharyngeal carcinoma cells(CNE-2) were treated with P(CS-g-mPEG-CA)CDs micelles at varying concentrations (0, 5, 10, 20, 25 and 50 μg/mL) for 72 h and the results are summarized in Fig. 8. It can be seen that the cell viability was 85.9% in the presence of blank micelles, indicating that P(CS-g-mPEG-CA) CDs was essentially nontoxic. The P(CS-g-mPEG-CA) CDs/DOX micelles exhibited dose- dependent cytotoxicity, and cell viability declined at higher drug concentrations. The results showed that all three self-assembled P(CS-g-mPEG-CA)CDs preparations had low cytotoxicity toward CNE-2 cells, indicating excellent biocompatibility. The results suggest that these drug-loaded micelles may have potential in cancer therapy.

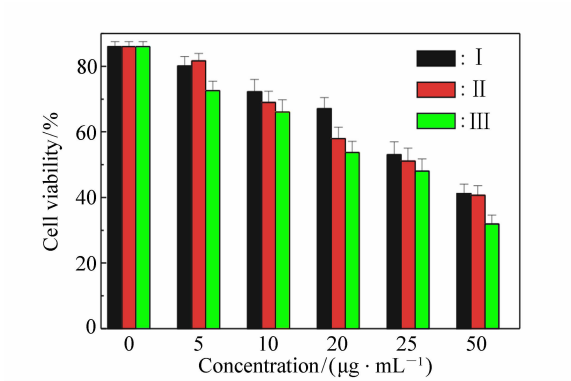

Fig. 8 Cell viability of the CNE-2 cells after incubation with the P(CS-g-mPEG-CA)CDs/DOX micelles for 72 h(n=3)

4 Conclusions

In this study, P(CS-g-mPEG-CA)CDs polymer carbon dots were successfully synthesized using a hydrothermal process as a new carrier material for drug delivery. The results of TEM and CMC analysis indicated that the synthesized P(CS-g-mPEG-CA)CDs could self-assemble into stable micelles with controlled size. A drug-loading study showed that the maximum entrapment efficiency of DOX was 40.8%, with maximum drug loading of 51.3%. Drug release was sustained over 400 h, with a maximum release of 28.7%. An MTT assay showed that drug-loaded polymer carbon dot micelles were cytotoxic toward CNE-2 cells. The P(CS-g-mPEG-CA) CDs can not only be loaded with a drug but also has fluorescent tracing properties, making it a good tracer drug carrier material. In addition, the P(CS-g-mPEG-CA) CDs has good application prospects in biomedical imaging, can support diagnosis and treatment of disease, and the surface molecules of P(CS-g-mPEG-CA)CDs can easily be modified to prepare multi-functional medical nano-particles to further expand its application.

参考文献:

[1] SUN Y P, ZHOU B, LIN Y, *et al.*. Quantum-sized carbon dots for bright and colorful photoluminescence[J]. *Journal of the American Chemical Society*, 2006, 128(24): 7756-7762.

[2] BAKER S N, BAKER G A. Luminescent carbon nanodots: emergent nanolights[J]. *Angewandte Chemie International Edition*, 2010, 49: 6726-6744.

[3] NIINO S, TAKESHITA S, ISO Y, *et al.*. Influence of chemical states of doped nitrogen on photoluminescence intensity of hydrothermally synthesized carbon dots[J]. *Journal of Luminescence*, 2016, 180: 123-131.

[4] 娄庆,曲松楠. 基于超级碳点的水致荧光"纳米炸弹"[J]. 中国光学,2015,8(1):91-98.
LOU Q,QU S N. Water triggered luminescent'nano-bombs'based on supra-carbon-nanodots[J]. *Chinese Optics*,2015,8(1):91-98. (in Chinese)

[5] HAN S,ZHANG H,XIE Y J,*et al.*. Application of cow milk-derived carbon dots/Ag NPs composite as the antibacterial agentn[J]. *Applied Surface Science*,2015,328:368-373.

[6] WANG C X,XU Z Z,CHENG H,*et al.*. A hydrothermal route to water-stable luminescent carbon dots as nanosensors for pH and temperature[J]. *Carbon*,2015,82:87-95.

[7] BARUAH U,GOGOI N,MAJUMDAR G,*et al.*. β-Cyclodextrin and calix [4] arene-25,26,27,28-tetrol capped carbon dots for selective and sensitive detection of fluoride[J]. *Carbohydrate Polymers*,2015,117:377-383.

[8] WANG W,CHENG L,LIU W. Biological applications of carbon dots[J]. *Science China Chemistry*,2014,57:522-539.

[9] YAO J,YANG M,DUAN Y. Chemistry, biology, and medicine of fluorescent nanomaterials and related systems: new insights into biosensing, bioimaging, genomics, diagnostics, and therapy[J]. *Chemical Reviews*,2014,114:6130-6148.

[10] XU X W,ZHANG K,ZHAO L,*et al.*. Aspirin-based Carbon dots, a good biocompatibility of material applied for bioimaging and anti-inflammation[J]. *ACS Appl. Mater. Interfaces*,2016,8:32706-32716.

[11] TAO S Y,SONG Y B,ZHU S J,*et al.*. A new type of polymer carbon dots with high quantum yield:from synthesis to investigation on fluorescence mechanism[J]. *Polymer*,2017,116:472-478.

[12] SONG G,LIN Y N,WANG H L. Strong fluorescence of poly(N-vinylpyrrolidone) and its oxidized hydrolysate[J]. *Macromolecular Rapid Communications*,2015,36:278-285.

[13] ZHU S J,SONG Y B,SHAO J R,*et al.*. Non-conjugated polymer dots with crosslink-enhanced emission in the absence of fluorophore units[J]. *Angewandte Chemie International Edition*,2015,47:14626-14637.

[14] YANG Y H,CUI J H,ZHENG M T,*et al.*. One-step synthesis of amino-functionalized fluorescent carbon nanoparticles by hydrothermal carbonization of chitosan[J]. *Chemical Communications*,2012,48:380-382.

[15] XIAO D L,YUAN D H,HE H,*et al.*. Microwave-assisted one-step green synthesis of amino-functionalized fluorescent carbon nitride dots from chitosan[J]. *Luminescence*,2013,28:612-615.

[16] WANG,Y F,WANG X,GENG Z H,*et al.*. Electrodeposition of a carbon dots/chitosan composite produced by a simple in situ method and electrically controlled release of carbon dots[J]. *Journal of Materials Chemistry B*,2015,3:7511-7517.

[17] ZU Y X,BI J R,YAN H P,*et al.*. Nanostructures derived from starch and chitosan for fluorescence bio-imaging[J]. *Nanomaterials*,2016,6:130-143.

[18] TANG Z J,LI G K,HU Y L. Advances in preparation and applications in quantitative analysis of nitrogen-doped carbon dots[J]. *Progress in Chemistry*,2016,28:1455-1461.

[19] LIN Y,ZHANG L Z,YAO W,*et al.*. Water-soluble chitosan-quantum dot hybrid nanospheres toward bioimaging and biolabeling[J]. *ACS Applied Materials & Interfaces*,2011,3:995-1002.

[20] WADAJKAR A S,KADAPURE T,ZHANG Y,*et al.*. Dual-imaging enabled cancer-targeting nanoparticles[J]. *Advanced Healthcare Materials*,2012,1:450-456.

[21] CHEN G,WANG L W,CORDIE T,*et al.*. Multi-functional self-fluorescent unimolecular micelles for tumor-targeted drug delivery and bioimaging[J]. *Biomaterials*,2015,47:41-50.

[22] WU D Q,LU B,CHANG C,*et al.*. Galactosylated fluorescent labeled micelles as a liver targeting drug carrier[J]. *Biomaterials*,2009,30:1363-1371.

[23] LEE Y K,HONG S M,KIM J S,*et al.*. Encapsulation of CdSe/ZnS quantum dots in poly(ethylene glycol)-Poly(D,L-lactide) micelle for biomedical imaging and detection[J]. *Macromolecular Research*,2007,15:330-336.

[24] SILL K,EMRICK T. Nitroxide-mediated radical polymerization from CdSe nanoparticles micelles[J]. *Chemistry of Materials*,2004,16:1240-1243.

[25] CHOWDHURI A R,TRIPATHY S,HALDAR C,*et al.*. Single step synthesis of carbon dot embedded chitosan nanoparticles for cell imaging and hydrophobic drug delivery[J]. *Journal of Materials Chemistry B*,2015,3:9122-9131.

[26] RADHAKUMARY C, NAIR P D, NAIR C P R, *et al.*. Chitosan-comb-graft-polyethylene glycol monomethacrylate-synthesis, characterization, and evaluation as a biomaterial for hemodialysis applications[J]. *Journal of Applied Polymer Science*, 2009, 114: 2873-2886.

[27] KONO H, TESHIROGI T. Cyclodextrin-grafted chitosan hydrogels for controlled drug delivery[J]. *International Journal of Biological Macromolecules*, 2015, 72: 299-308.

[28] GEDDA G, LEE C Y, LIN Y C, *et al.*. Green synthesis of carbon dots from prawn shells for highly selective and sensitive detection of copper ions[J]. *Sensors and Actuators B: Chemical*, 2016, 224: 396-403.

[29] FU D J, JIN Y, XIE M Q, *et al.*. Preparation and characterization of mPEG grafted chitosan micelles as 5-fluorouracil carriers for effective anti-tumor activity[J]. *Chinese Chemical Letters*, 2014, 25: 1435-1440.

[30] PAPADIMITRIOU S A, ACHILIAS D S, BIKIARIS D N. Chitosan-g-PEG nanoparticles ionically crosslinked with poly (glutamic acid) and tripolyphosphate as protein delivery systems[J]. *International Journal of Pharmaceutics*, 2012, 430: 318-327.

[31] LI X Y, KONG X Y, SHI S, *et al.*. Biodegradable MPEG-g-chitosan and methoxy poly(ethylene glycol)-b-poly(e-caprolactone) composite films: Part 1. preparation and characterization[J]. *Carbohydrate Polymers*, 2010, 79: 429-436.

[32] ZHANG Y, WANG Y L, FENG X T, *et al.*. Effect of reaction temperature on structure and fluorescence properties of nitrogen-doped carbon dots[J]. *Applied Surface Science*, 2016, 387: 1236-1246.

[33] YANG S W, SUN, J, LI X B, *et al.*. Large-scale fabrication of heavy doped carbon quantum dots with tunable-photoluminescence and sensitive fluorescence detection[J]. *Journal of Materials Chemistry A*, 2014, 2: 8660-8667.

[34] ARDEKANI S M, DEHGHANI A, HASSAN M, *et al.*. Two-photon excitation triggers combined chemo-photothermal therapy via doped carbon nanohybrid dots for effective breast cancer treatment[J]. *Chemical Engineering Journal*, 2017, 330: 651-662.

[35] FAN R J, SUN Q, ZHANG L, *et al.*. Photoluminescent carbon dots directly derived from polyethylene glycol and their application for cellular imaging[J]. *Carbon*, 2014, 71: 87-93.

[36] REMANT K B C, THAPA B, XU P S. pH and redox dual responsive nanoparticle for nuclear targeted drug delivery[J]. *Molecular Pharmaceutics*, 2012, 9: 2719-2729.

作者简介：

于淑娟(1977—)，女，吉林长春人，博士，副教授，硕士研究生导师，2001 年、2004 年于长春工业大学分别获得学士、硕士学位，2007 年于大连理工大学获得博士学位，主要从事荧光碳纳米材料、高分子光稳定剂的合成与应用性能方面的研究。E-mail: ysj2007@126.com